

1  
6  
7  
7



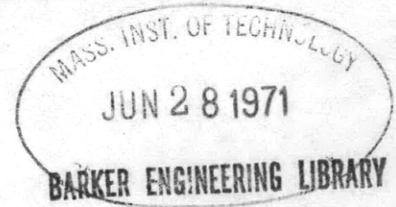
AD 422 190

STRUCTURAL DEVELOPMENT OF A TITANIUM  
OCEANOGRAPHIC VEHICLE FOR OPERATING  
DEPTHS OF 15,000 TO 20,000 FEET

Martin A. Krenzke, et al

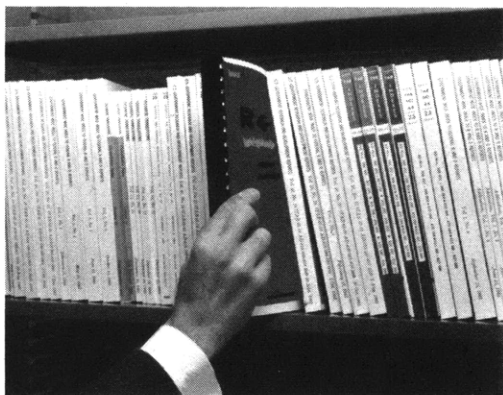
David Taylor Model Basin  
Washington, D. C.

September 1963



DISTRIBUTED BY:

**CLEARINGHOUSE**  
FOR FEDERAL SCIENTIFIC AND TECHNICAL INFORMATION



## REPORT selection aids

*Pinpointing R & D reports for industry*

Clearinghouse, Springfield, Va. 22151

**U.S. GOVERNMENT RESEARCH AND DEVELOPMENT REPORTS (USGRDR)---**SEMI-MONTHLY JOURNAL ANNOUNCING R&D REPORTS. ANNUAL SUBSCRIPTION \$30.00 (\$37.50 FOREIGN MAILING). SINGLE COPY \$3.00.

**U.S. GOVERNMENT RESEARCH AND DEVELOPMENT REPORTS INDEX---**SEMI-MONTHLY INDEX TO U.S. GOVERNMENT RESEARCH AND DEVELOPMENT REPORTS. ANNUAL SUBSCRIPTION \$22.00 (\$27.50 FOREIGN MAILING). SINGLE COPY \$3.00.

**FAST ANNOUNCEMENT SERVICE---**SUMMARIES OF SELECTED R&D REPORTS COMPILED AND MAILED BY SUBJECT CATEGORIES. ANNUAL SUBSCRIPTION \$5.00, TWO YEARS: \$9.00, AND THREE YEARS: \$12.00. WRITE FOR AN APPLICATION FORM.

**DOCUMENT PRICES---**ALMOST ALL OF THE DOCUMENTS IN THE CLEARINGHOUSE COLLECTION ARE PRICED AT \$3.00 FOR PAPER COPIES AND 65 CENTS FOR COPIES IN MICROFICHE.

**COUPONS---**THE CLEARINGHOUSE PREPAID DOCUMENT COUPON SALES SYSTEM FOR PURCHASING PAPER COPIES AND MICROFICHE PROVIDES FASTER, MORE EFFICIENT SERVICE ON DOCUMENT REQUESTS. THE PREPAID COUPON IS A TABULATING CARD WITH A FACE VALUE OF THE PURCHASE PRICE OF A CLEARINGHOUSE DOCUMENT (\$3.00 PAPER COPY OR 65 CENTS MICROFICHE). IT IS YOUR METHOD OF PAYMENT, ORDER FORM, SHIPPING LABEL, AND RECEIPT OF SALE.

COUPONS FOR PAPER COPY (HC) DOCUMENTS ARE AVAILABLE AT \$3.00 EACH OR IN BOOKS OF 10 COUPONS FOR \$30.00. COUPONS FOR MICROFICHE COPIES OF CLEARINGHOUSE DOCUMENTS ARE AVAILABLE IN BOOKS OF 50 COUPONS FOR \$32.50. WRITE FOR A COUPON ORDER FORM.

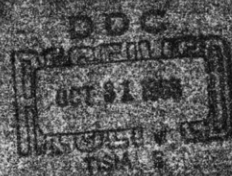
AD No. 422190



DEPARTMENT OF THE NAVY

STRUCTURAL DEVELOPMENT OF A TITANIUM  
OCEANOGRAPHIC VEHICLE FOR OPERATING  
DEPTHS OF 15,000 TO 20,000 FEET

Martin A. Krenzke  
and  
Thomas J. Kieman



STRUCTURAL MECHANICS LABORATORY  
RESEARCH AND DEVELOPMENT REPORT

September 1963

Report 1677

HYDROMECHANICS

AERODYNAMICS

STRUCTURAL  
MECHANICS

APPLIED  
MATHEMATICS

STRUCTURAL DEVELOPMENT OF A TITANIUM  
OCEANOGRAPHIC VEHICLE FOR OPERATING  
DEPTHS OF 15,000 TO 20,000 FEET

by  
Martin A. Krenzke  
and  
Thomas J. Kieman

September 1963

Report 1677  
S-F013 01 03

## TABLE OF CONTENTS

	Page
ABSTRACT .....	1
INTRODUCTION.....	1
DESIGN CONCEPTS .....	3
JACKET MATERIAL WITH HIGHER MODULUS OF ELASTICITY.	4
JACKET AND RING MATERIAL WITH SAME MODULUS OF ELASTICITY .....	5
JACKET MATERIAL WITH LOWER MODULUS OF ELASTICITY.	6
DESCRIPTION OF MODELS .....	7
MODEL DSRV-3 .....	12
MODEL DSRV-3L.....	14
MODELS DSRV-3C AND DSRV-3CP.....	18
TEST PROCEDURE.....	20
TEST RESULTS.....	26
DISCUSSION .....	35
CONCLUSIONS.....	46
RECOMMENDATIONS.....	47
ACKNOWLEDGMENTS.....	47
APPENDIX - HYDROSTATIC TEST OF A SMALL STIFFENED ALUMINUM CYLINDER .....	49
REFERENCES .....	57

## LIST OF FIGURES

	Page
Figure 1 - Distribution of Ocean Depth .....	2
Figure 2 - Stress-Pressure Diagram for Composite Hull of Weldable Steel Jacket and Titanium Rings.....	4
Figure 3 - Stress-Pressure Diagram for Composite Hull of Weldable Titanium Jacket and Titanium Rings.....	6
Figure 4 - Stress-Pressure Diagram for Composite Hull of Fiberglass Jacket and Titanium Rings.....	7
Figure 5 - Models DSRV-3, DSRV-3L, DSRV-3C, and DSRV-3CP.	8
Figure 6 - Typical Stress-Strain Curves for Titanium Alloys Used in Models .....	9
Figure 7 - Schematic Sketch of an Oceanographic Vehicle With a 9-Foot Outer Diameter.....	11
Figure 8 - Various Stages in the Fabrication of Model DSRV-3...	13
Figure 9 - Fusion Welding of 1/32-Inch-Titanium Jacket .....	17
Figure 10 - Chamber Used for Welding of Model DSRV-3L.....	19
Figure 11 - Model DSRV-3L before Test.....	20
Figure 12 - Models DSRV-3C and DSRV-3CP after Fabrication .....	21
Figure 13 - Strain-Gage Locations .....	22
Figure 14 - Models after Test.....	27
Figure 15 - Typical Plots of Pressure against Strain.....	30
Figure 16 - Extrapolated Collapse Depth versus Yield Strength of Titanium Ring Material for Model DSRV-3L Hull Geometry .....	40
Figure 17 - Model DSRV-P.....	50
Figure 18 - Typical Stress-Strain Curve for Material Used in Model DSRV-P.....	50



LIST OF FIGURES (Cont'd)	
	Page
Figure 19 - Model DSRV-P after Collapse .....	51

LIST OF TABLES	
Table 1 - Ratio of Theoretical Collapse Pressures to Experimental Collapse Pressures .....	37
Table 2 - Estimated Ratio of Weight of Pressure Hull to Weight of Displacement for Various Composite Titanium Hulls.....	42
Table 3 - Ratio of Theoretical Collapse Pressure to Experimental Collapse Pressure for Model DSRV-P.....	52

## ABSTRACT

This report presents the structural development of a titanium oceanographic vehicle capable of operating at depths of 15,000 to 20,000 ft. Emphasis is placed on the utilization of current titanium technology in the construction of the vehicle. To assist in the development, four titanium models were designed, fabricated according to feasible full-scale techniques, and tested to failure under external hydrostatic pressure. Based on the test results, estimates are made of the ratio of weight to displacement required for titanium pressure hulls with collapse depths to 30,000 ft. The need to fabricate full-scale "trial manufacturing" sections to definitely establish feasibility is emphasized.

## INTRODUCTION

Considerable interest has recently been shown in manned vehicles capable of exploring the depths of the ocean. A glance at Figure 1 shows that 60 to 98 percent of the ocean floor could be explored by manned vehicles capable of operating at depths of 15,000 to 20,000 ft.

The structural design of the hull of such a vehicle must consider strength-to-weight ratios of possible hull materials and the relation between structural weight (or depth) and payload. The steels currently in use are too heavy for consideration as hull materials. Thus, the designer must introduce new materials such as high-strength aluminum,

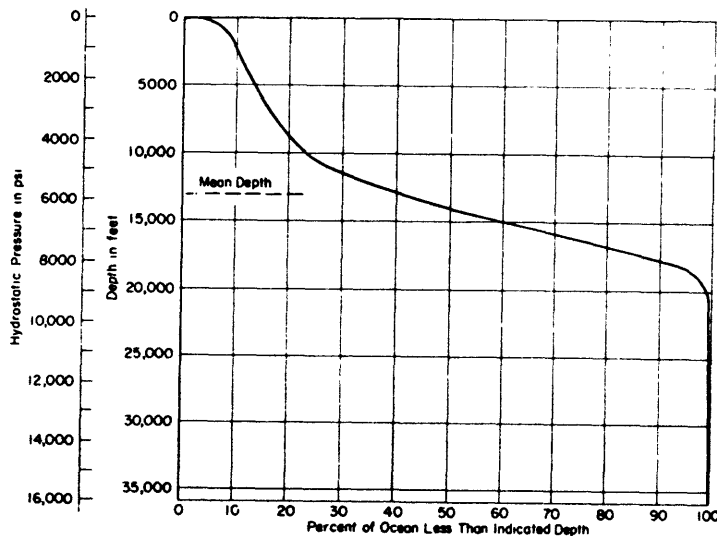


Figure 1 - Distribution of Ocean Depth

beryllium, fiberglass, titanium, or super strength steels. Since welding techniques for some of these new materials have not yet been developed, new methods of construction must also be considered.

High-strength titanium is one of the most promising new hull materials. It weighs approximately 276 lb/cu ft compared to a weight of 490 lb/cu ft for steel. Some alloys with yield strengths of 120,000 psi may currently be welded in thin sheets if extreme care is used to prevent contamination. Nonweldable alloys with yield strengths to 175,000 psi and greater are also available.

This report presents the structural development of a titanium oceanographic vehicle with collapse depths to 30,000 ft; discusses the use of composite construction; and on the basis of model test results, presents estimates of the strength-weight characteristics of composite titanium pressure hulls.

### DESIGN CONCEPTS

A composite pressure hull as referred to in this report, is composed of cylindrical segments, not physically joined together, placed inside a relatively thin jacket. The cylindrical segments are designed to resist loads due to the external hydrostatic pressure, whereas the function of the jacket is to provide watertight integrity, longitudinal strength to resist bending moments occurring when surfaced, and corrosive protection for the strength elements. The chief advantage is that composite construction eliminates the need to weld or join the basic hull structures. The material used in the cylindrical segments may be chosen for its high strength-to-weight ratio, and the material used in the jacket is normally selected for its relative ease of fabrication and its resistance to salt water environment.

Various combinations of materials with compatible yield strengths and moduli of elasticity may be used in the construction of composite pressure hulls. The principle will be demonstrated for three typical combinations.

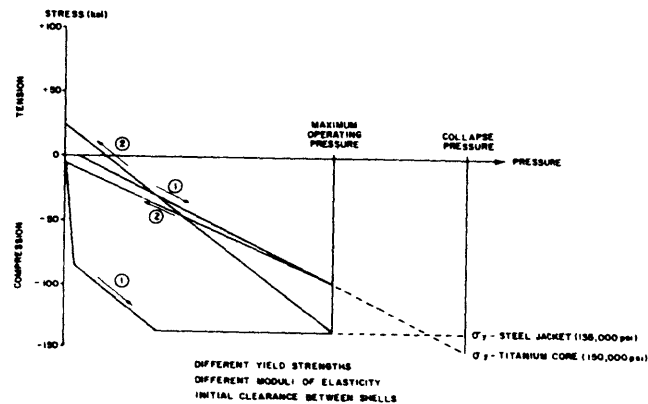


Figure 2 - Stress-Pressure Diagram for Composite Hull of Weldable Steel Jacket and Titanium Rings

#### JACKET MATERIAL WITH HIGHER MODULUS OF ELASTICITY

Figure 2 is a stress-pressure diagram for a composite hull of HY-135 steel and a high-strength titanium alloy with steel; the material with the higher modulus of elasticity, is used as the jacket material. Here it is assumed that there is an initial clearance between the steel jacket and the titanium segments. During the initial application of pressure, the steel of the jacket follows Curve 1 and is stressed to its yield point at a relatively low pressure. As further pressure is applied, the steel flows plastically and remains stressed at 135,000 psi (if strain hardening effects are neglected) and transmits the pressure load to the titanium. Upon release of pressure, the two materials act together. Because of the differences in moduli of elasticity, the steel follows the steeper Curve 2

and the titanium follows the less steep Curve 2. Therefore, at zero pressure, the steel jacket is in a state of residual tension and the titanium is in a state of residual compression. The magnitude of these residual stresses depends on the relative yield strengths of the titanium and steel, the geometry of the hull, and the maximum pressure applied. It is not dependent upon the magnitude of initial clearance between jacket and rings as long as the Bauschinger<sup>1</sup> effect is negligible. Although it is assumed in Figure 2 that there is an initial clearance between the steel and titanium, these same materials may be used with no initial clearance or with the steel preshrunk around the titanium.

#### JACKET AND RING MATERIAL WITH SAME MODULUS OF ELASTICITY

A second combination of compatible materials, high-strength titanium segments inside a lower strength, weldable titanium jacket, is demonstrated in Figure 3. It is assumed that there is no initial clearance between the jacket and core; therefore, as pressure is initially applied, both the jacket and the ring segments follow the same Curve 1 (because their moduli of elasticity are the same) until the stress in the lower strength jacket reaches its yield point. If strain-hardening effects are neglected, the jacket continues to yield at the same stress as the pressure is increased, but the cylindrical segments are stressed at an increased rate since they are carrying a larger percentage of the pressure. When the pressure is released, the two hulls function as a unit.

<sup>1</sup> References are listed on page 57.

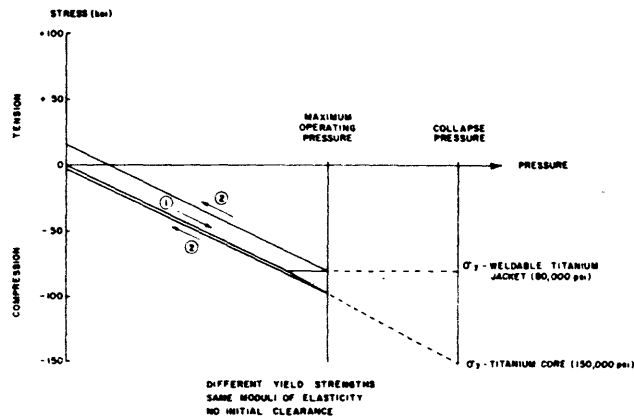


Figure 3 - Stress-Pressure Diagram for Composite Hull of Weldable Titanium Jacket and Titanium Rings

The stress in the jacket follows the upper Curve 2, and that in the inner segments follows the lower Curve 2, resulting in a residual tension in the weldable titanium jacket and a slight residual compression in the high-strength, inner segments at zero pressure.

#### JACKET MATERIAL WITH LOWER MODULUS OF ELASTICITY

Figure 4 demonstrates the third principle of composite construction for fiberglass and titanium where the material in the jacket has the lower modulus. Because of the fabrication technique, the fiberglass jacket has an initial tension which holds the nonweldable cylindrical titanium segments in place. The two shells function together at all times, and all stresses are elastic. As the pressure is applied and released, the

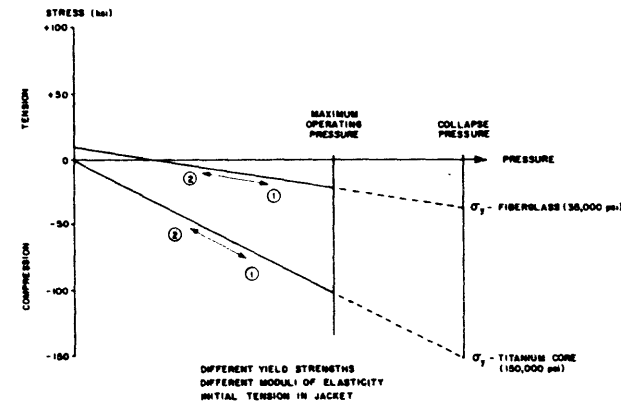


Figure 4 - Stress-Pressure Diagram for Composite Hull of Fiberglass Jacket and Titanium Rings

stresses in the fiberglass jacket follow the upper curve and those in the titanium rings follow the lower curve.

#### DESCRIPTION OF MODELS

The four models reported in this investigation are designated DSRV-3, DSRV-3L, DSRV-3C and DSRV-3CP. Sketches of the models are shown in Figure 5, and representative stress-strain curves for the titanium alloys used in the fabrication of the models are presented in Figure 6.

Model geometries were determined for a projected oceanographic vehicle with an outside diameter of 9 ft and a collapse depth of 30,000 ft. A schematic sketch showing prototype geometries and yield strength requirements is presented in Figure 7.

Figure 5 - Models DSRV-3, DSRV-3L, DSRV-3C, and DSRV-3CP

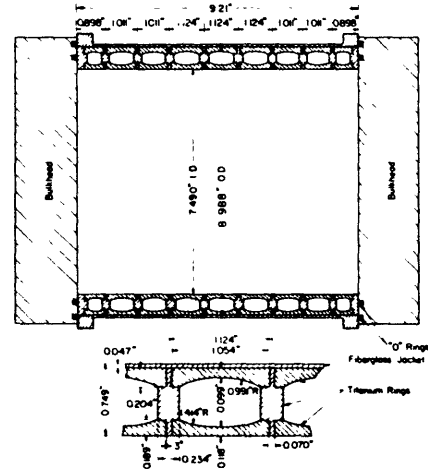


Figure 5a - Model DSRV-3

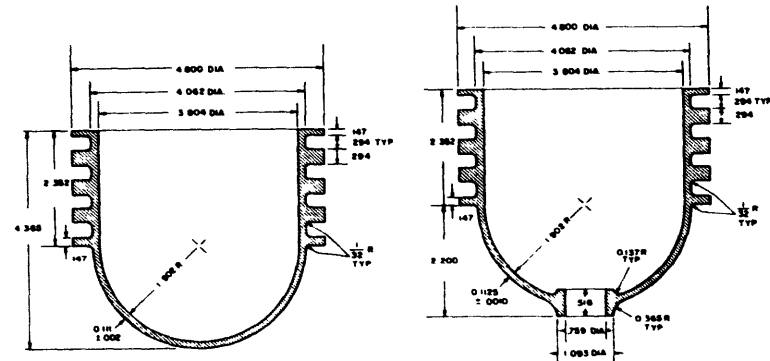


Figure 5c - Model DSRV-3C      Figure 5d - Model DSRV-3CP

Figure 6 - Typical Stress-Strain Curves for Titanium Alloys Used in Models

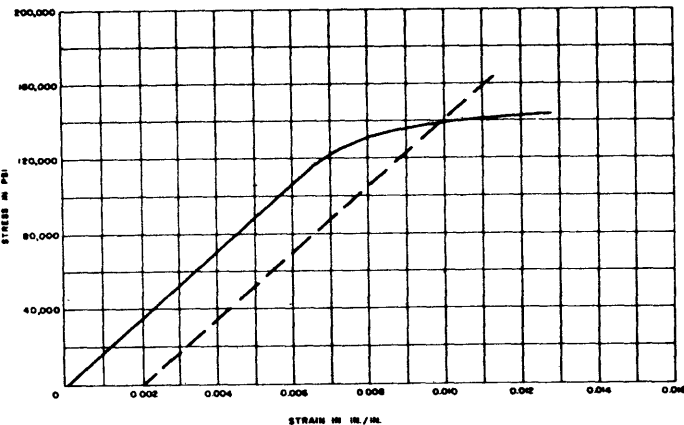


Figure 6a - Model DSRV-3

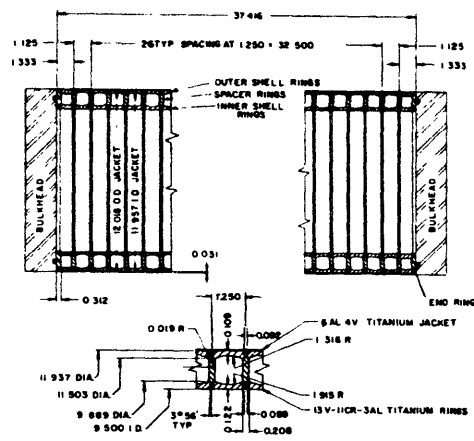


Figure 5b - Model DSRV-3L



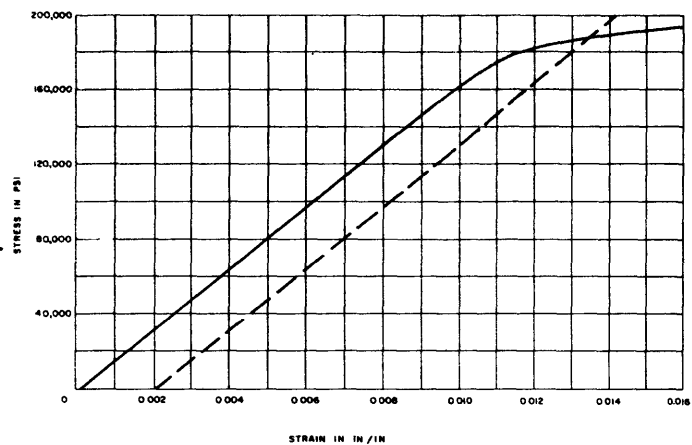


Figure 6b - Model DSRV-3L

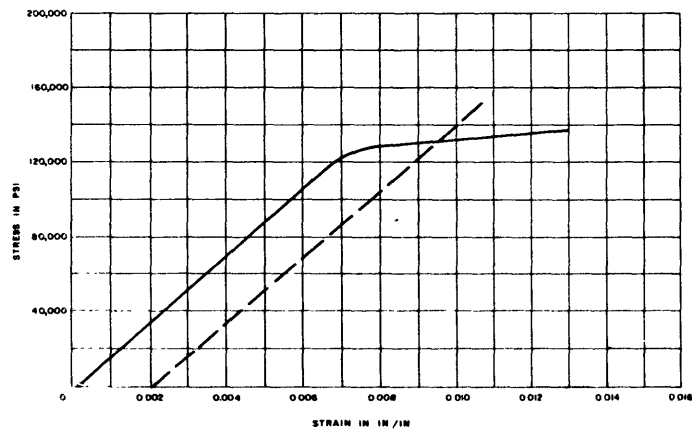


Figure 6c - Models DSRV-3C and DSRV-3CP

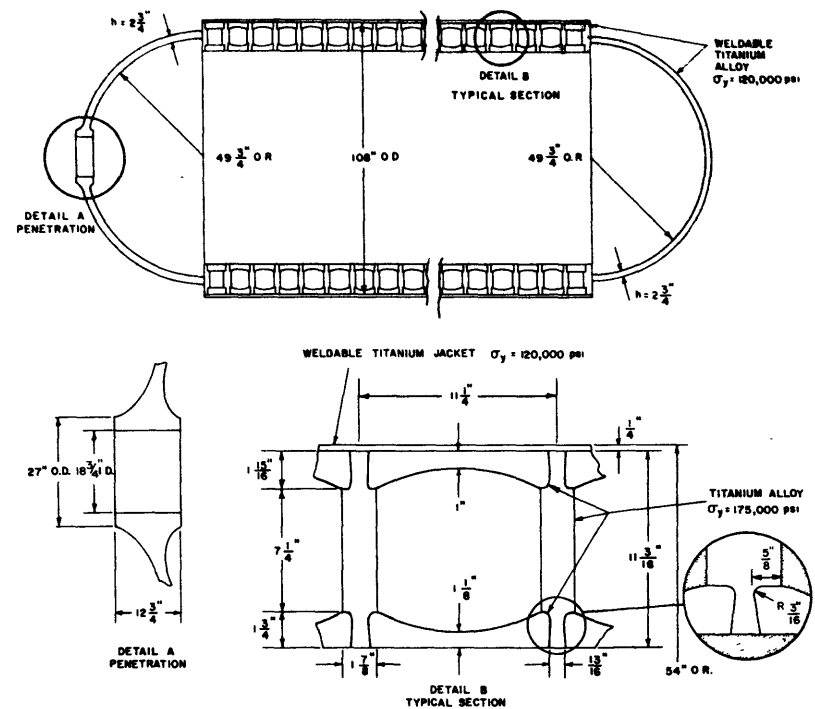


Figure 7 - Schematic Sketch of an Oceanographic Vehicle With a 9-Foot Outer Diameter

Since this was primarily an investigation of hydrostatic strength, it should be emphasized that the criteria used for the selection of the titanium alloys for the models were simply those of strength and weldability. The alloys used in the fabrication of the models are not necessarily those which would be recommended for a prototype vehicle.

#### MODEL DSRV-3

Model DSRV-3 is a membrane sandwich composite cylinder about 1 diameter in length. This rather exploratory model was designed to study the strength of a typical bay of a composite hull fabricated from a titanium alloy with a yield strength of 150,000 psi.\* In designing the typical bay, the two-dimensional Hencky-Von Mises stress intensity<sup>2</sup> on all the material was arbitrarily allowed to reach 95 percent of the yield strength. Longitudinal bending stresses were eliminated by varying the thickness of the shell rings.<sup>3</sup> Fiberglass was chosen as the material for the jacket since it provided a simple solution to the problem of sealing the cylinder for test purposes. The ratio of weight of material to weight of displacement for a typical section of the model was 0.67.\*\*

The titanium rings were machined from forged tubes of 6Al4V titanium. A fiberglass jacket, composed of 50-percent glass content cloth together with epoxy resin was hand wrapped tightly around the assembled titanium rings. Photographs of various stages in the fabrication of the model are shown in Figure 8.

\* All yield strengths presented in this report are compressive yield strengths (0.2 percent offset). All specimens were tested at a rate of 250 psi/min beyond the proportional limit. An effort was made to load the models at approximately the same rate as the specimens.

\*\* A density of 276 lb/cu ft was used for titanium in the computations of displacement ratios for all four models.

Figure 8 - Various Stages in the Fabrication of Model DSRV-3

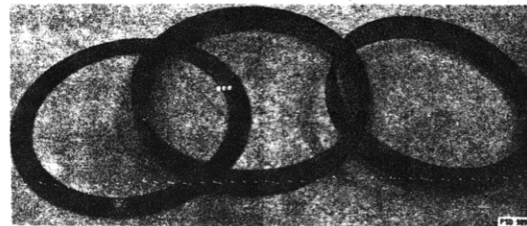


Figure 8a - Typical Ring Elements

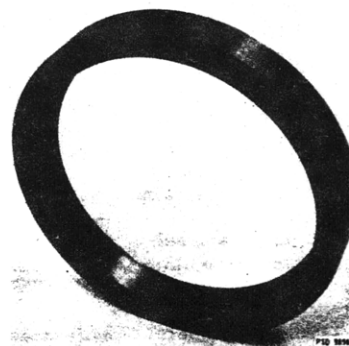


Figure 8b - Typical Ring Assembly

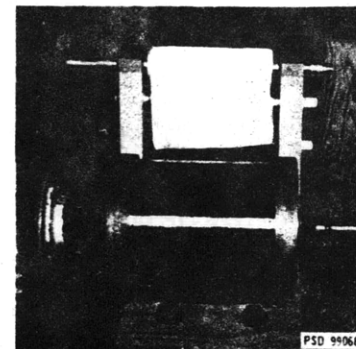


Figure 8c - Complete Ring Assembly Prepared for Fiberglass Jacket

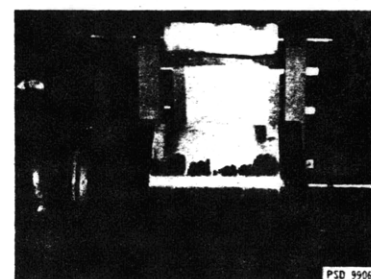


Figure 8d - Initial Stage Jacket Layup

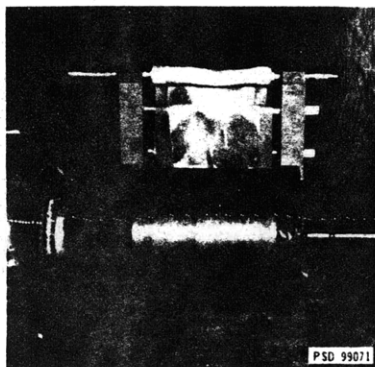


Figure 8e - Final Stage of Jacket Layup

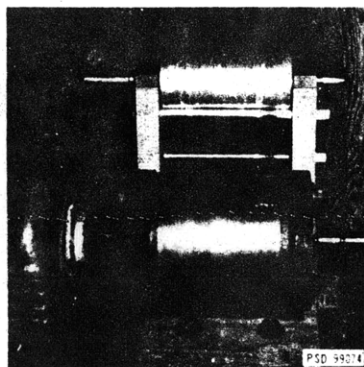


Figure 8f - Layup of Sealing Surface

#### MODEL DSRV-3L

Model DSRV-3L is a membrane sandwich cylinder approximately 3 diameters in length. The design of this model was based on the test results of Model DSRV-3 and was intended to produce a conservative estimate of the collapse strength of the assumed semi-infinite cylindrical portion of the projected prototype hull shown in Figure 7.

It was concluded from the results of Model DSRV-3 that a long sandwich cylinder with similar typical bay geometry would collapse in the plastic general-instability mode. This conclusion was supported by results of the test of a small ring-stiffened cylinder. (These results are presented in the Appendix.)

The plastic general-instability collapse strength depends on the ratio of the critical elastic buckling stress to the stress at collapse. To

ensure a conservative interpretation of test results, it is therefore necessary that for a particular model test, this ratio be held as low as the minimum ratio which may be encountered in the prototype. In Model DSRV-3L, this was accomplished in two ways:

1. The critical buckling stress in the elastic general-instability mode was minimized by
  - a. designing a cylinder of sufficient length to simulate a semi-infinite cylinder and
  - b. selecting a hull material with a low Young's modulus.
2. A material with a yield strength of 175,000 psi was chosen to produce a relatively high stress at collapse. At present this yield strength is considered to be an upper bound.

Since the actual stress-strain curves for the material to be used in the model were not available for design purposes, the average circumferential stress of a typical section was allowed to reach the yield strength at a depth of 30,000 ft. Model DSRV-3 test results had indicated that this would be a conservative approach. To improve the fatigue strength of the jacket and to ensure that the inner and outer segments acted as a structural unit in the plastic range, bending stresses were eliminated in the inner and outer shell rings by varying the thickness of the rings.<sup>3</sup> A weldable titanium alloy with a yield strength of approximately 120,000 psi was chosen as the material for the jacket and end rings. The ratio of weight of material to weight of displacement for a typical section was 0.62.

Two titanium alloys were used in manufacturing Model DSRV-3L. Because of its weldability, solution annealed 6Al4V titanium with a yield strength of 140,000 psi was chosen for the jacket and end rings. The inner and outer rings and the spacer rings were machined from 13V11Cr3Al titanium forgings aged to ensure the required yield strengths. Some difficulty was encountered in fabricating the 1/32-in. jacket. A preliminary test sheet, 12 in. long, was successfully rolled to the proper diameter. Attempts to roll a sheet 36 in. long were unsuccessful, however, and the jacket was finally formed by pressing. An allowance of approximately 0.010 in. was made in the circumferential length of the cylinder for shrinkage due to welding. This value was determined by welds made on test strips of 6Al4V titanium. After forming, the cylinder was carefully aligned in a longitudinal seam jig. The edges of the cylinder were butted together in a fixture, the cylinder was clamped along its entire length, and the joint was fusion-welded by machine; see Figure 9.

The inner and outer rings and the spacer rings were machined from forged rings in the heat-treated condition and with a Rockwell Hardness number of C46. Based on preliminary tests of small forging samples, the forgings for the spacer rings were aged at  $900\text{ F} \pm 5^\circ$  for 60 hr. A ductility of 3 percent was obtained on tests of specimens from an extra forging included in the heat for test purposes. This was considerably less than the 8-percent ductility of the samples. The forgings for the inner and outer shell rings were aged at 900 F for 40 hr in an

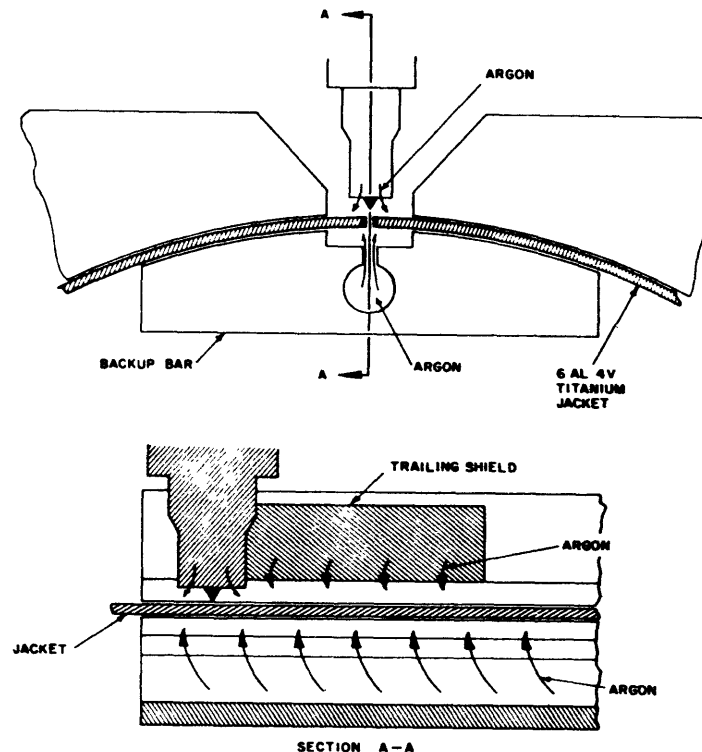


Figure 9 - Fusion Welding of 1/32-Inch Titanium Jacket

unsuccessful attempt to improve the ductility. The reduction in ductility is attributed to the working of the rings during forging. The stress-strain

curve of Figure 6b was determined from tests of specimens taken from the extra forgings included in the heats.

The end rings were machined from 3/8-in. plate in the solution annealed condition. After machining, the rings were slipped inside the jacket. This operation was facilitated by the initial diametrical clearance of 0.020 in. between the outer rings and the jacket. The assembled model was then placed in a sealed atmosphere; see Figure 10. Air was bled from the system as argon was supplied over a 24-hr period. A 6A14V filter wire was used in welding the jacket to the end rings.

Photographs of the model before test are shown in Figure 11. Note the irregular surface of the jacket caused by the manufacturing operation.

#### MODELS DSRV-3C AND DSRV-3CP

Models DSRV-3C and DSRV-3CP were designed to study the collapse strength of machined titanium hemispherical end closures with and without penetrations. Since stress-strain curves were not available for design purposes, the average stress in the hemisphere was allowed to reach 120,000 psi at a collapse depth of 30,000 ft. To avoid the additional cost involved in fabricating a composite cylinder to provide boundaries to the hemisphere, monolithic cylinder-hemisphere structures were used. The cylinders were designed to provide membrane boundary conditions for the hemispheres.<sup>4</sup> The reinforcement for the penetration of Model DSRV-3CP was also designed to provide a membrane boundary condition.<sup>4</sup>

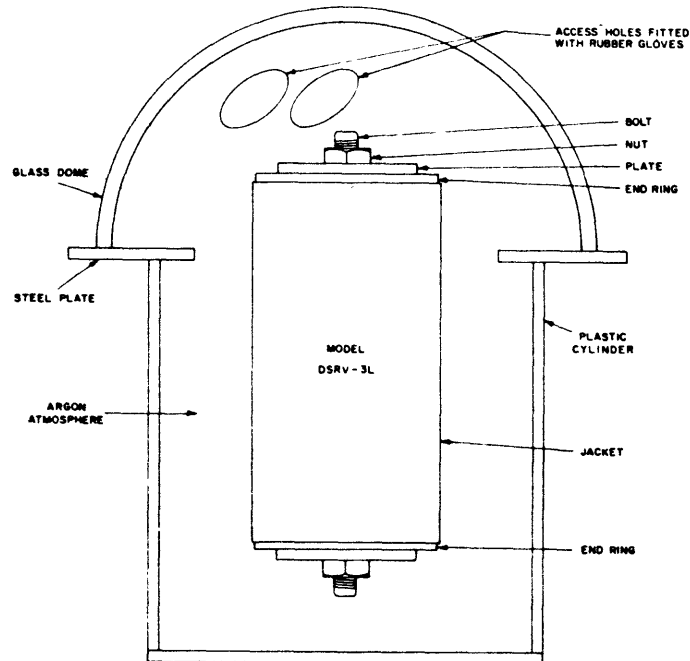


Figure 10 - Chamber Used for Welding of Model DSRV-3L

This resulted in the replacement of 153 percent of the removed cross-sectional area. The weight of material to weight of displacement for the hemispheres was 0.68.

The models were machined from a 5-in. diameter annealed forging of 6A14V titanium. Photographs of the models after fabrication are shown in Figure 12.



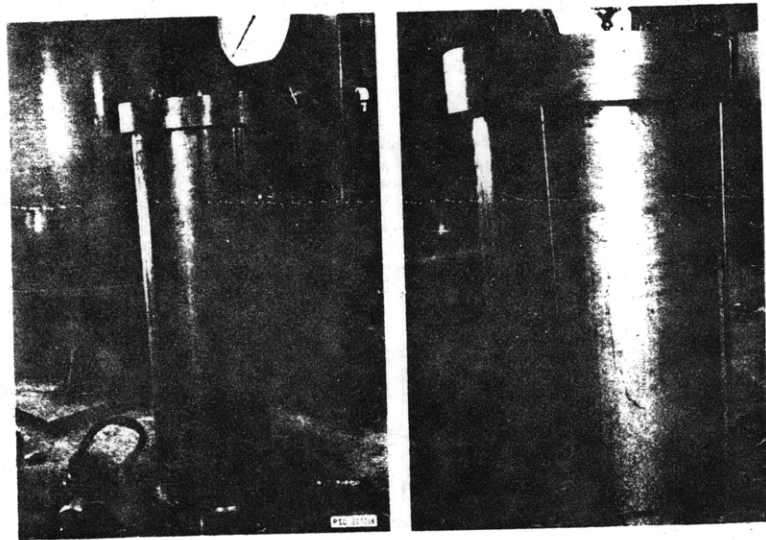


Figure 11 - Model DSRV-3L before Test

#### TEST PROCEDURE

Foil-resistance strain gages were used to measure strains in the longitudinal and circumferential directions of each model. Gages were located to indicate the strain distribution along the length of the models as well as around the circumference. Gage locations are shown in the diagrams of Figure 13.

Since facilities with sufficient pressure capacity were not available on station in the early stages of this investigation, several tanks were used in testing Model DSRV-3. The model was subjected to a pressure of 3000 psi in the 10-in.-diameter pressure tank at the Taylor Model

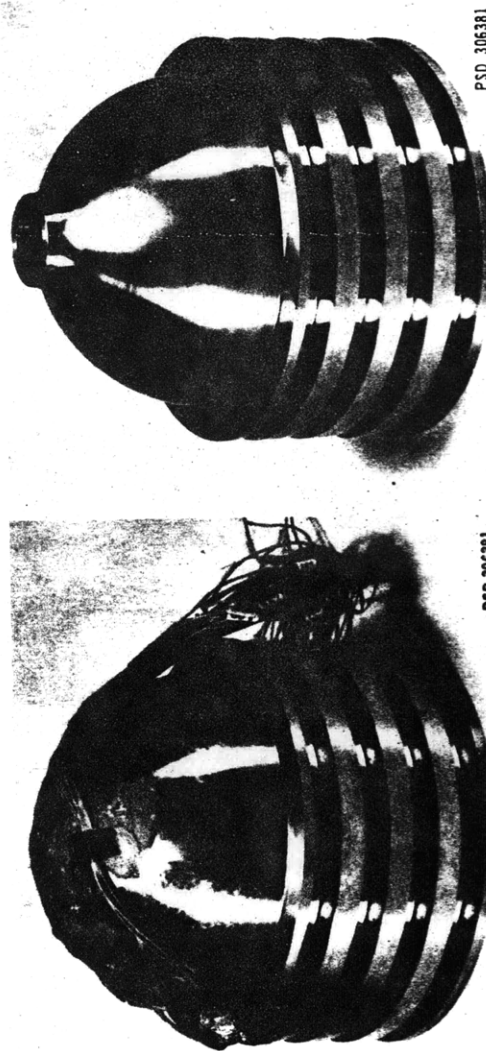


Figure 12a - Model DSRV-3C  
Note: After instrumentation.

Figure 12b - Model DSRV-3CP

Figure 12 - Models DSRV-3C and DSRV-3CP after Fabrication

Figure 13 - Strain-Gage Locations

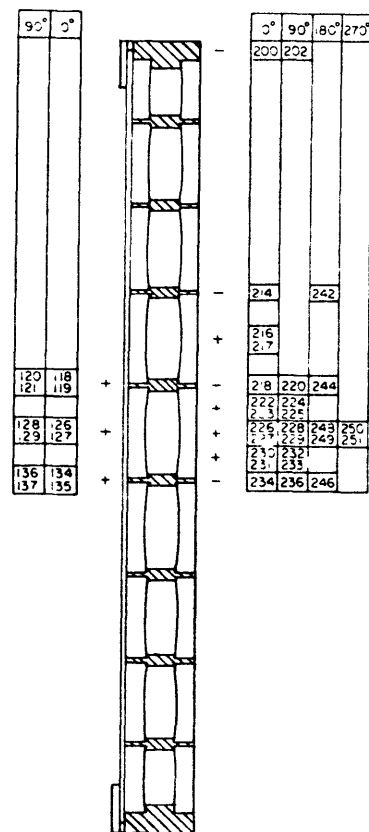


Figure 13a - Model DSRV-3

Note: All even-numbered gages measured circumferential strain.  
All exterior gages have numbers in the 100 series; all interior gages in the 200 series.

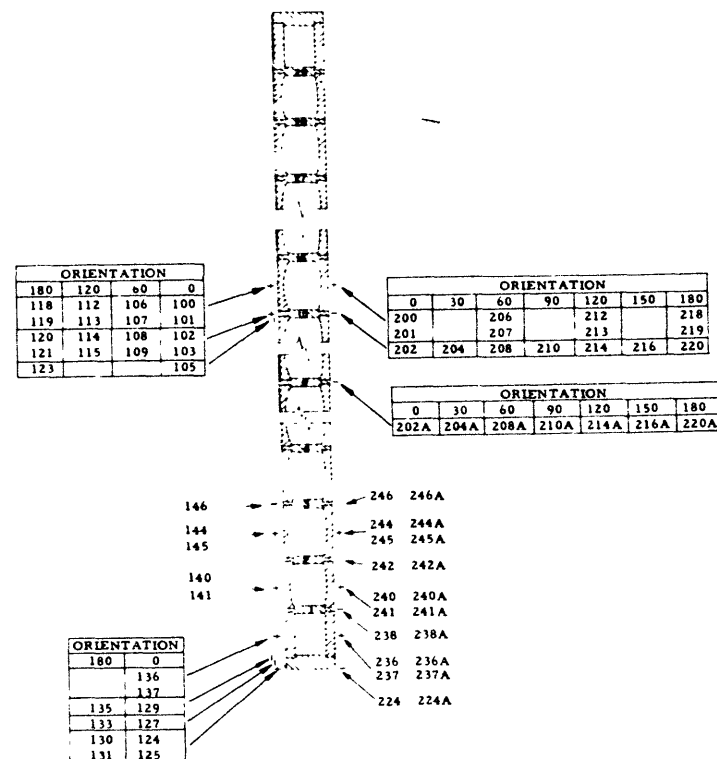


Figure 13b - Model DSRV-3L

Note: The letter A indicates gages placed on the model during reinstrumentation after the third of five runs.



Models DSRV-3C and DSRV-3CP were tested to collapse in the Model Basin 5-in.-diameter high-pressure tank. Oil was used as the pressure medium, and internal and external strains were recorded to collapse. All of the external gages could not be recorded during the same pressure run since only a limited number of leads could be brought out of the tank.

#### TEST RESULTS

Models DSRV-3, DSRV-3C, and DSRV-3CP collapsed at pressures of 14,250, 14,000, and 14,700 psi, respectively. Model DSRV-3L failed at a pressure of 15,750 psi. When the model reached this pressure, the strains began to run and the pressure fell off slowly. The pressure was then released so that the model could be used for future dynamic studies. Measurements on the model after test indicated a maximum variation in diameter of 1/16 in. in the  $n = 2$  mode. Photographs of the models after test are shown in Figure 14.

During the test of Model DSRV-3L no buckling was observed in the jacket when the model was removed from the tank for visual inspection. Figure 14a shows the extent to which the jacket yielded around the high-strength shell rings. The irregular surface, shown in Figure 11, has disappeared and the location of the shell rings can be determined from the circumferential outlines apparent in the photograph.

Pressure-strain data for all four models are plotted in Figure 15. Strain sensitivities, the initial slope of the pressure-strain plots, for Models DSRV-3C and DSRV-3CP are tabulated in Figures 13c and 13d.

Figure 14 - Models after Test



Figure 14a - Portions of Model DSRV-3

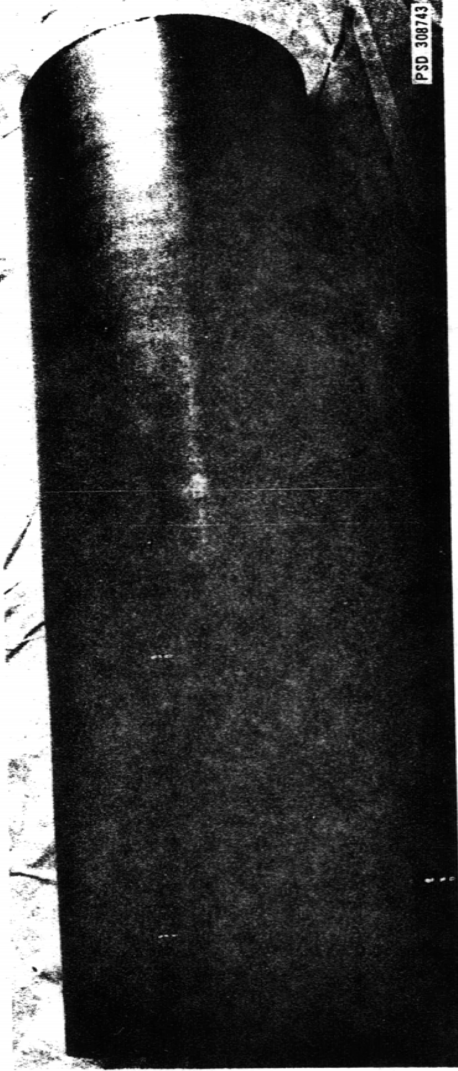


Figure 14b - Model DSRV-3L

412190

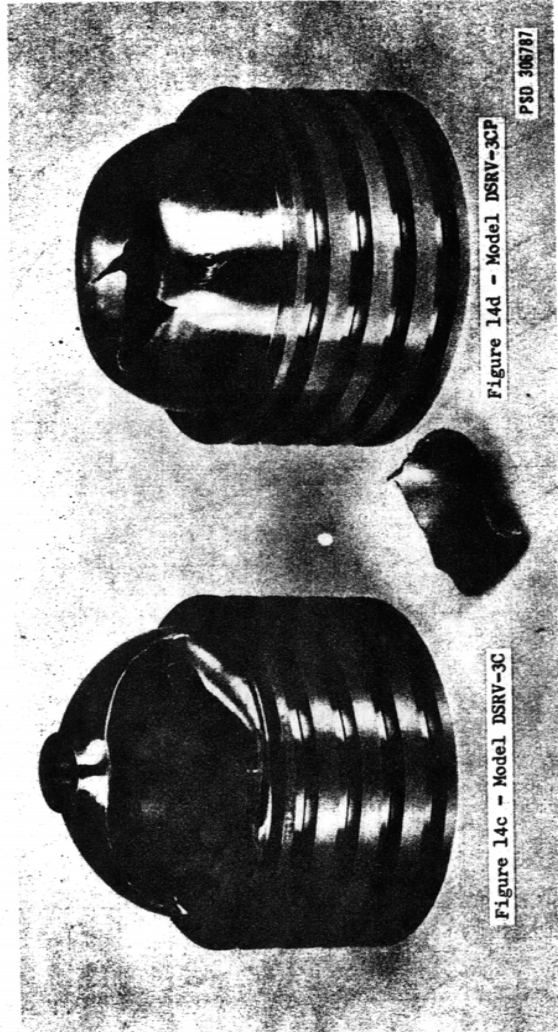
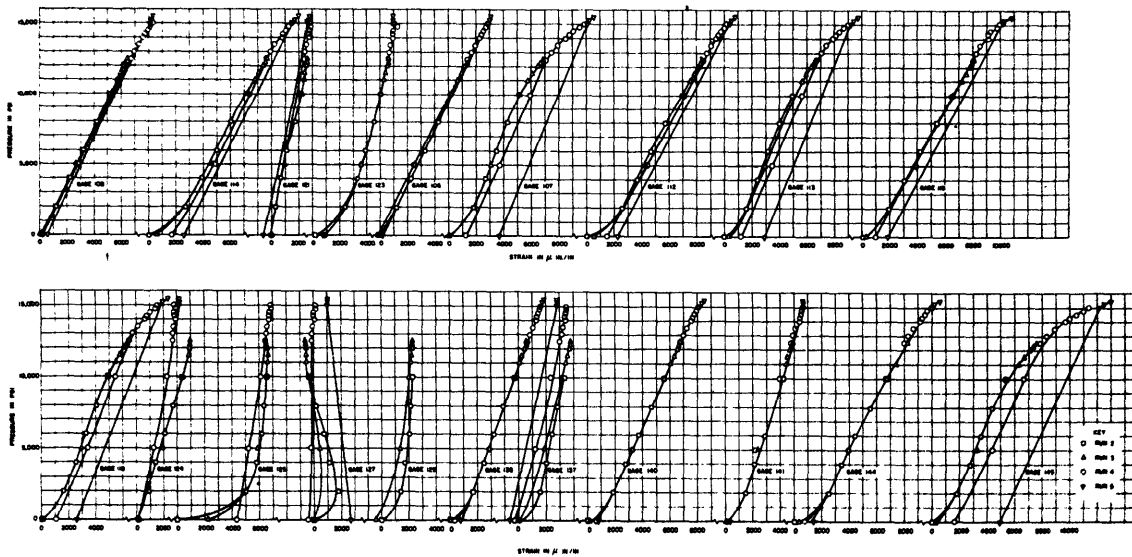
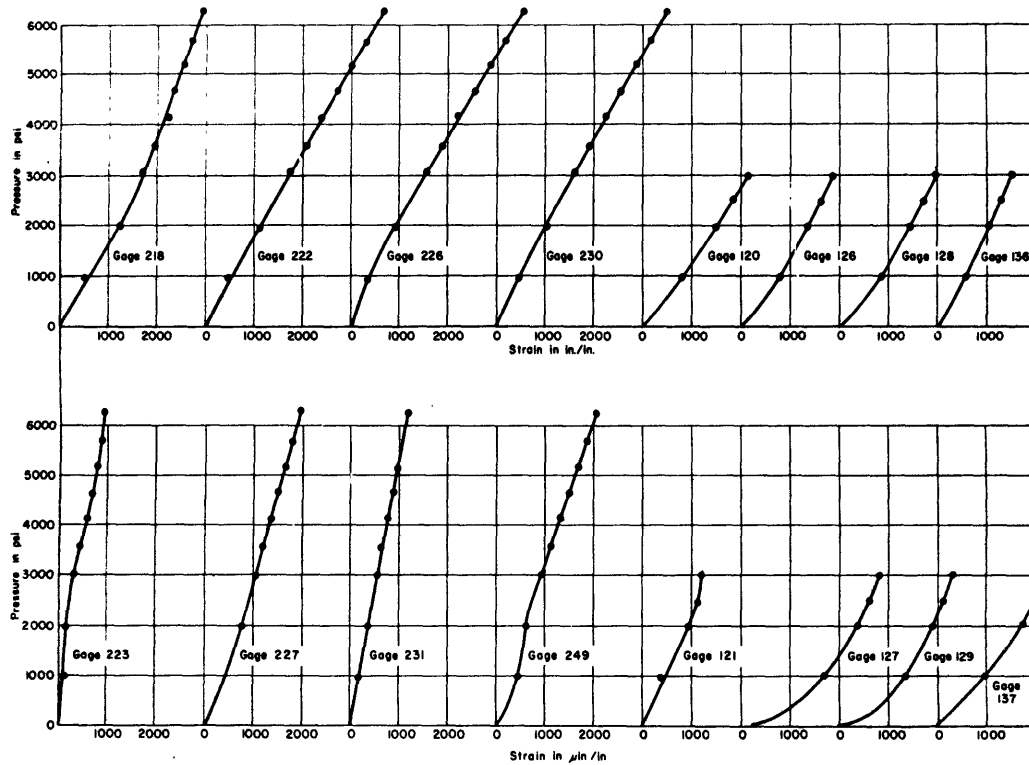




Figure 15 - Typical Plots of Pressure against Strain



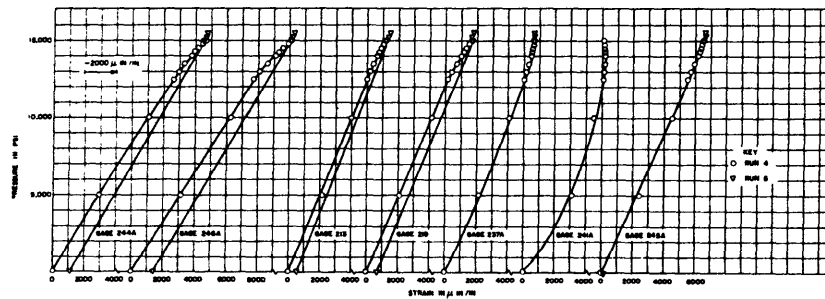
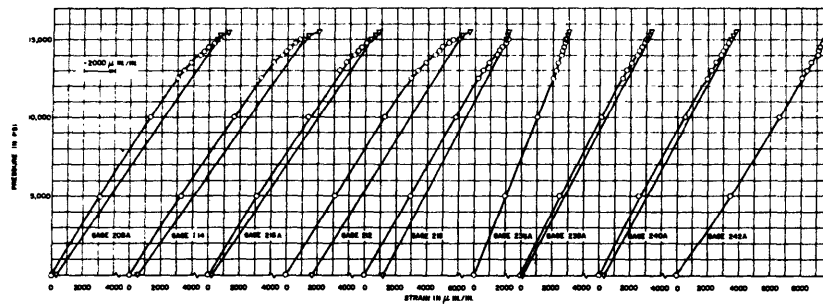


Figure 15c - Model DSRV-3L

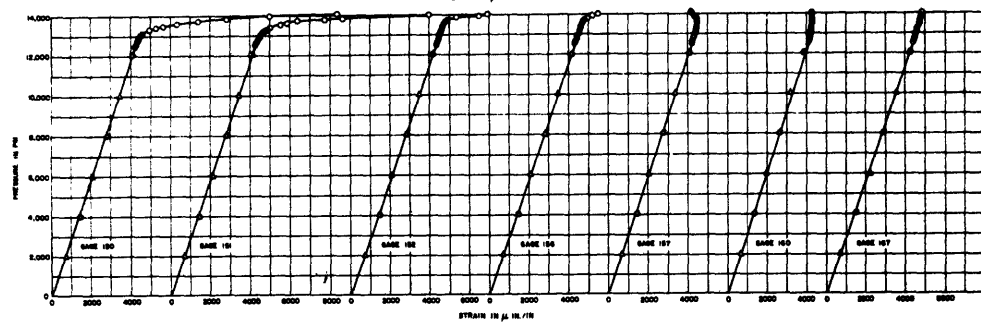
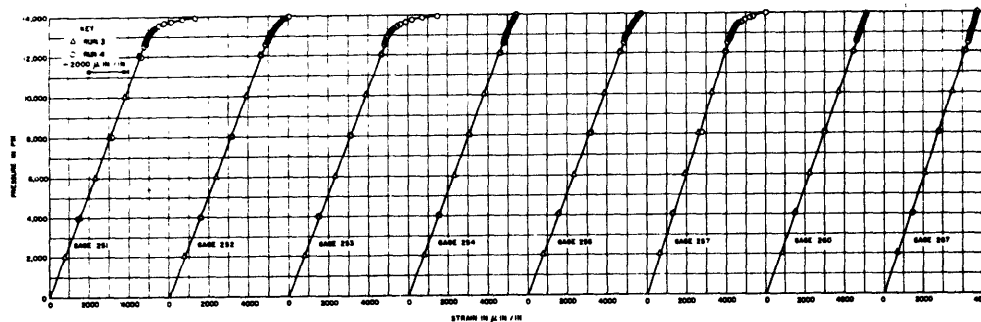


Figure 15d - Model DSRV-3C

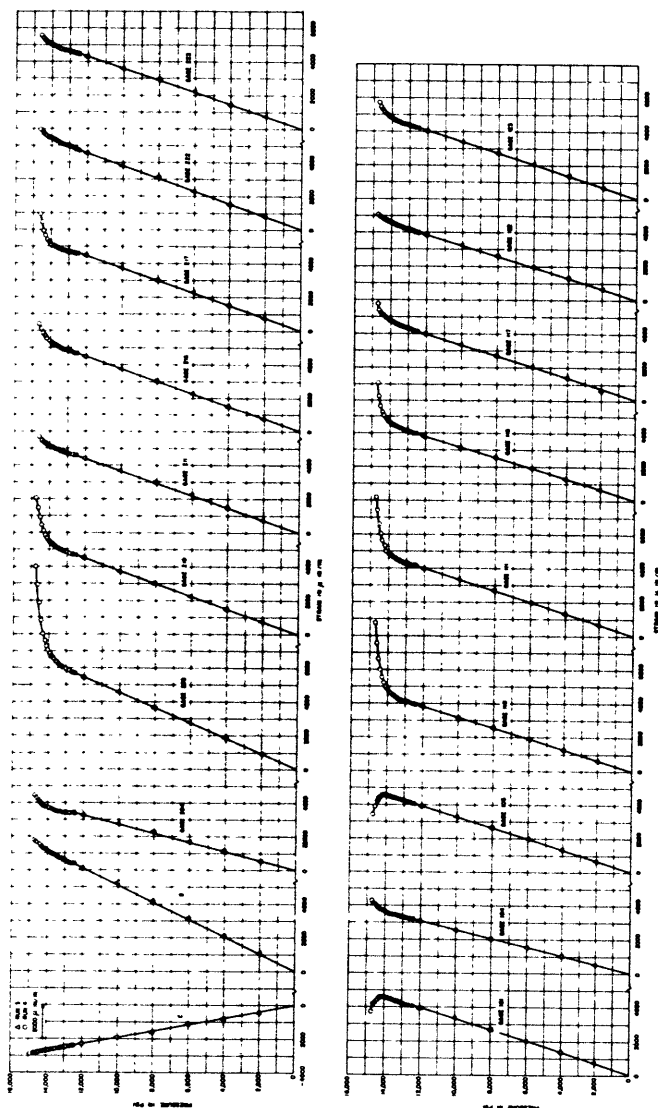


Figure 15e - Model DSRV-3CP

## DISCUSSION

Stresses in each model at collapse were well into the plastic range of the material. Model DSRV-3 apparently failed in the plastic general-instability mode. No strain data were recorded near collapse pressure during the test of DSRV-3, and the model was extensively damaged. Thus there is no positive proof as to the actual mode of collapse. However, the appearance of several of the rings after collapse indicated that collapse occurred by general instability in the  $n = 2$  mode. Model DSRV-3L definitely failed by plastic general instability; this is demonstrated by the measured out-of-round shape after completion of the test and by the bifurcation of recorded circumferential strains as shown in Figure 15. Models DSRV-3C and DSRV-3CP each failed by plastic buckling of the hemispherical portion.

Prior to the design and test of these models, no reliable theories were available with which to predict the plastic general-instability strength of stiffened cylinders and the plastic buckling strength of deep spherical shells.\* Therefore, exploratory tests were conducted on a machined ring-stiffened cylinder which failed in the plastic general-instability mode and on a series of machined aluminum hemispheres which failed in both

\* Bijlaard developed a theory for the plastic buckling of spherical shells in 1949.<sup>5</sup> At the time Model DSRV-3C was designed, no experimental results were available with which to check the validity of his work. However, there was reason to believe that a design based on his theory would not be conservative since it reduces to the classical small deflection theory in the elastic range.

the elastic and inelastic buckling modes. The results of the cylinder test are incorporated in the Appendix, and the hemispherical test results are summarized in Reference 6.

Semi-empirical design equations for machined shells were developed for both modes of collapse. The pressures calculated using these equations are compared with the present results in Table 1. Excellent agreement between experiment and the applicable design equation was obtained for each model.

Several assumptions were necessary to compute the plastic general instability pressure for Models DSRV-3 and DSRV-3L. On the basis of relative moduli and yield strength the fiberglass jacket of Model DSRV-3 was considered to be equivalent to one of titanium one-fourth the actual thickness. For Model DSRV-3L, the titanium jacket was considered to reduce the pressure acting on the segments by a pressure equal to that which causes yielding of the unsupported jacket according to the Hencky-Von Mises yield criterion.

The elastic strains obtained for each model in areas not affected by boundary conditions were in reasonable agreement with theory. The average experimental strains obtained from gages in typical bay locations of Model DSRV-3 were within 6 percent of the theoretical strains predicted by the theory of Reference 3. With the exception of the longitudinal strains in the jacket, the strains measured in Model DSRV-3L were also in reasonable agreement with calculated strains.<sup>2</sup> However, the

TABLE 1

Model	Experimental Collapse Pressure psi	Mode of Collapse	Design Equation	Calculated Collapse Pressure psi	Ratio of Theoretical Collapse Pressures to Experimental Collapse Pressures	
					Theoretical Collapse Pressure	Experimental Collapse Pressure
DSRV-3	14,250	Plastic General Instability	Equation [9], Appendix	14,800	0.97	
DSRV-3L	15,750	Plastic General Instability	Equation [9], Appendix	15,300	0.97	
DSRV-3C	14,000	Plastic Instability (Spherical Portion)	Equation [14], Reference 6	14,200	1.01	
DSRV-3CP	14,700	Plastic Instability (Spherical Portion)	Equation [14], Reference 6	14,300	0.97	

longitudinal strains in the jacket were higher than the calculated values at the frame and somewhat lower than the calculated value at midbay. The experimental strains in areas of DSRV-3C and DSRV-3CP away from the boundary cylinder and, in the case of DSRV-3CP, away from the penetration were in excellent agreement with those strains associated with equilibrium considerations.

The cylinders of Models DSRV-3C and DSRV-3CP and, in the case of Model DSRV-3CP, the penetration reinforcement provided ideal, membrane boundary conditions for the spherical portions of these models consistent with the design concepts used.<sup>4</sup> The measured strains demonstrate that no appreciable bending occurred in any areas of the spherical portions of these models; see Figures 13c and 13d.

No special attention had been given to boundary conditions when designing Models DSRV-3 and DSRV-3L. However, from the limited amount of strain data recorded in areas adjacent to the bulkheads on Model DSRV-3L, it appears that the radial deflection of the end rings was slightly less than the membrane deflection of a hemispherical end closure as represented by Models DSRV-3C and DSRV-3CP. Therefore, the strain distribution obtained near the ends of Model DSRV-3L appears to be a realistic representation of those which would occur if it had been terminated by hemispherical closures similar to DSRV-3C and if the junctures had been designed to provide membrane boundary condition to the hemisphere. Since the magnitude of the measured strains near the

ends of Model DSRV-3L are not severe, it appears that the design of the inner and outer shells and of the stiffened spacing at each end is adequate. However, the friction between the end stiffener and the flat bulkhead undoubtedly restricted radial deflection at that point. Theoretical calculations<sup>4</sup> required to determine the geometry of an intersection between the cylinder and the hemispherical end closure would show whether additional area is needed in the end ring.

A considerable amount of creep occurred during the test of each model; strains, which were recorded at intervals throughout the test of each model except DSRV-3, continued to drift as data were recorded in the latter stages of each test. The collapse pressure of each model was influenced by the rate at which pressure was applied, just as the shape of the stress-strain curve and the 0.2-percent offset yield of a simple compression specimen is influenced by the rate at which load is applied.<sup>7</sup> Therefore, extreme caution should be used when designing a titanium hull to withstand pressure for a long-time duration to ensure adequate consideration of the effects of rate of load application.

The relationship between estimated collapse depth and the yield strength of the inner rings for cylindrical hulls of the same geometry and, therefore, the same weight-to-displacement ratio as Model DSRV-3L is shown in Figure 16. It has been assumed that each alloy has the same strain-hardening characteristics and that the yield strength of the jacket material is two-thirds that of the inner ring material. Since ring



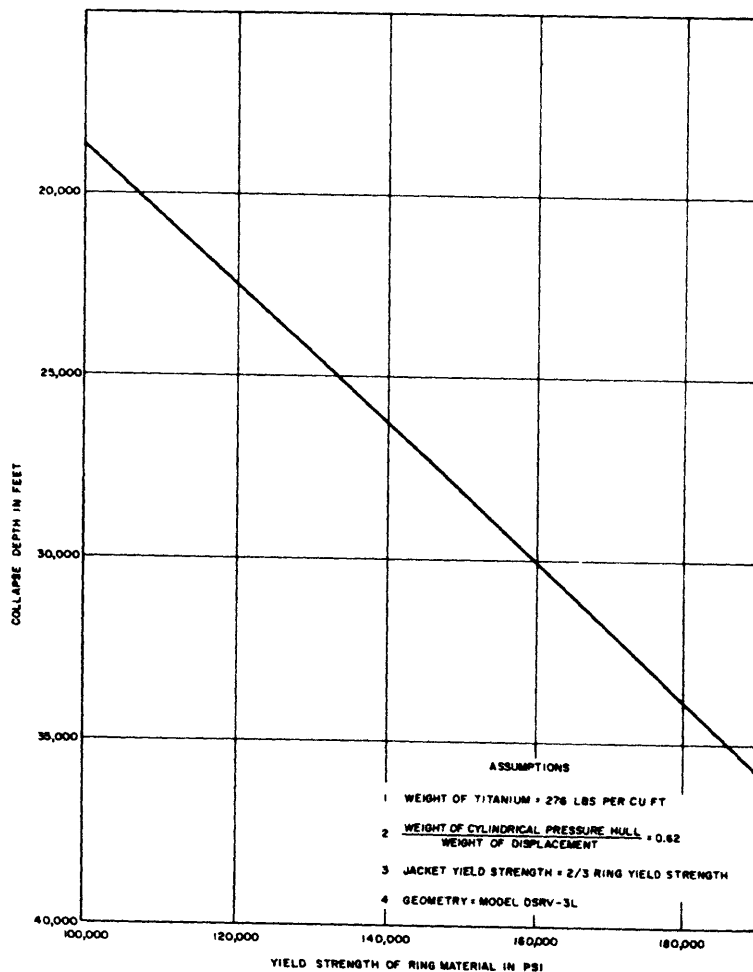


Figure 16 - Extrapolated Collapse Depth versus Yield Strength of Titanium Ring Material for Model DSRV-3L Hull Geometry

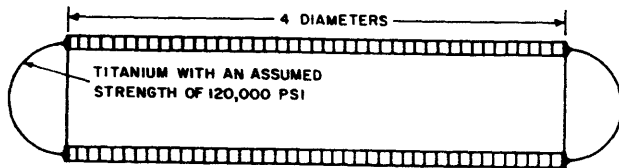
material of 189,000 psi was used in Model DSRV-3L, the estimates of collapse depth shown in Figure 16 for titanium alloys of lower yield strengths should be conservative.

Table 2 presents the ratios of weight of total pressure hull to weight of its displacement in sea water for composite titanium hull with various yield strengths and for collapse depths of 22,500, 27,000, and 30,000 ft. These ratios are based on the results of these tests adjusted linearly to account for differences in collapse depth, hull weight, and material yield strengths. The pressure hull is assumed to consist of a cylinder 4 diameters in length and terminated on either end by titanium hemispherical end closures with an assumed yield strength of 120,000 psi. In all weight calculations, the geometry of the juncture of hemisphere with cylinder was assumed to be similar to that represented by the end ring and adjacent sandwich structure present in Model DSRV-3L. It is interesting to note that ALUMINAUT, which has a design collapse depth of about 22,500 ft,\* has a ratio of weight of hull to weight of displacement of about 0.75. Table 2 shows that collapse depths of 22,500 ft may be obtained with considerably lower weight displacement ratios by using high-strength titanium alloys as the principal hull material. Specifically, it may be concluded that the proposed ALUMINAUT pressure hull weighs about 40 percent more than the estimated weight of a composite titanium hull designed for the same collapse depth and composed of HY-100

\* ALUMINAUT has a design operating depth of 15,000 ft with an assumed factor of safety of 1.5.

TABLE 2

Estimated Ratio of Weight of Pressure Hull to Weight of Displacement for Various Composite Titanium Hulls



Yield Strength of Material Used in Rings psi	Yield Strength of Material Used in Jacket psi	Collapse Depth ft	Weight of Pressure Hull / Weight of Displacement
120,000	80,000	22,500	0.63
120,000	80,000	27,000	0.75
120,000	80,000	30,000	0.83
150,000	100,000	22,500	0.52*
150,000	100,000	27,000	0.62
150,000	100,000	30,000	0.69
175,000	120,000	27,000	0.55**
175,000	120,000	30,000	0.60
200,000	120,000	30,000	0.55**

\* Not conservative since ratios of weight of hull to weight of displacement for both calculated cylindrical and hemispherical shells are considerably less than those of DSRV-3L and DSRV-3C from which this value was extrapolated.

\*\* Not conservative since ratio of weight of cylindrical hull to weight of its displacement is considerably less than that of DSRV-3L from which this value was extrapolated.

titanium jacket and HY-150 titanium rings. Corresponding conclusions may be drawn from Table 2 for other collapse depths and material yield strengths.

Various methods of producing the high-strength titanium rings required for composite construction appear feasible. For relatively small diameters, the complete rings could be forged in a manner similar to that used in Model DSRV-3L. Recent developments in diffusion bonding offer a method of joining segments of a ring to form large complete rings. For example, segments of annealed 6Al4V titanium alloy could be joined by diffusion bonding to form a complete ring and could then be heat-treated to strength levels of 150,000 psi and greater. Several titanium alloys with a yield strength of 120,000 psi, such as the 6Al4V and 721 alloys, show promise of being weldable under favorable conditions. Complete rings of these materials could, therefore, be formed by welding segments together. When a "weldable" titanium alloy is used as the ring material, composite construction offers the advantage of eliminating many of the difficult and time-consuming weldments such as those joining the web and shells. Although composite construction will undoubtedly require machining of the individual rings, it is likely that considerable machining of fully welded titanium hulls will also be required to obtain proper welding conditions.

Each main structural element was machined for this series of models. However, several conclusions may be reached concerning hulls of similar

geometry fabricated by other means, such as by forming and welding plates or by diffusion bonding machined elements. If performed at room temperature, welding and forming operations will give rise to considerable residual stresses which, in turn, will cause an early nonlinear pressure-strain relationship to occur. For the depths studied in this series of tests, collapse strength of both cylindrical and spherical titanium alloy hulls are affected by this relationship, and a corresponding decrease in collapse pressure can be expected for hulls fabricated by this method. Further nonlinearity and an associated decrease in collapse strength can be expected if initial imperfections are present due to fabrication. These initial imperfections may be severe in both the welded as well as the diffusion-bonded hulls, where very high temperatures are required during the bonding operation. The effect of both residual stresses and initial imperfections on collapse strength will be particularly noticeable in the hemispherical end closures. Therefore, if these results are used to predict collapse strength of hulls of similar geometry but assembled by different fabrication procedures, careful consideration should be given to the possible effects of residual stresses and initial imperfections. Since these effects are almost entirely eliminated in composite cylinders, it is possible that the structural efficiency of cylinders fabricated according to this method is greater than that of cylinders fabricated by the standard method of fully welded construction.

Hull penetration, cylinder-end closure junctures, fatigue strength, and methods of attaching machinery foundations require investigation before a deep-depth oceanographic vehicle of composite construction may be accomplished. Recent Model Basin tests of small-scale composite aluminum cylinders indicate that satisfactory hull penetrations, end closures, and fatigue strength may be achieved. However, realistic large-scale models with penetrations and end closures must be tested under both static and cyclic loading to confirm these preliminary conclusions before sufficient confidence may be placed in a prototype design. Methods of attaching foundations to a composite hull must be developed, particularly if the inner rings are nonweldable. A successful solution to this problem is anticipated since the shock requirements would most likely be very nominal.

It appears that the most severe obstacle to attaining a deep-depth vehicle is the development of full-scale fabrication techniques. Composite construction offers a promising solution to this problem. However, as in the case of a welded titanium hull, construction of a full-scale, "trial manufacturing" section is considered mandatory before the feasibility of a prototype may be definitely established. Such a "trial manufacturing" section should include a portion of cylinder with representative rings, an end closure, and an associated juncture. Each of these segments would also provide useful information for a welded titanium sandwich hull in the event that advances in technology permit this

type of construction. This is particularly true of the end closures which, at this time, present a very difficult fabrication problem, regardless of which method of joining is considered. If titanium welding technology is not developed, the possibility exists that a steel jacket and steel end closures may be substituted for the titanium jacket and end closures considered in this report. However, this would result in a weight penalty which might be severe for hulls with low length-to-diameter ratios.

#### CONCLUSIONS

1. A titanium hull composed of a composite cylinder with an HY-120 jacket and HY-175 inner rings and terminated by machined HY-120 hemispheres would weigh approximately 60 percent of its displacement, when designed for a collapse depth of 30,000 ft. Similarly, hulls composed chiefly of HY-150 or HY-120 rings would weigh about 55 or 63 percent of their displacement, respectively, when designed for a collapse depth of 22,500 ft. Further estimates are summarized in Table 2.

2. The collapse strengths of the cylindrical Models DSRV-3 and DSRV-3L are predicted by a semi-empirical equation developed in the Appendix for plastic general instability. The collapse strengths of the hemispherical portions of Models DSRV-3C and DSRV-3CP are predicted by Equation [14] of Reference 6 for the plastic buckling of machined deep spherical shells.

3. The hydrostatic collapse strength of titanium hulls depends on the rate at which the load is applied.

4. Composite construction shows promise of enabling the use of present high-strength titanium alloys and associated technology in the design of deep-depth oceanographic vehicles.

5. Before definite conclusions can be reached regarding the feasibility of a titanium deep-depth vehicle, large-scale models with realistic penetrations and end closures should be tested under static and cyclic loading and a full-scale "trial manufacturing" section, including end closures, should be fabricated.

#### RECOMMENDATIONS

1. The hydrostatic and fatigue strength of titanium hulls with realistic penetrations and end closures and constructed according to feasible full-scale fabrication procedures should be investigated.

2. Methods of attaching machinery foundations to composite hulls should be developed.

3. A full-scale, "trial-manufacturing" section of a composite titanium oceanographic vehicle should be fabricated to demonstrate feasibility.

4. The effect of creep on the collapse strength of titanium hulls should be investigated.

#### ACKNOWLEDGMENTS

The authors wish to express their appreciation to Mr. R. D. Short for developing the membrane theory for cylindrical shells used in the design of these models, to Mr. A. R. Willner for providing guidance on the material aspects of this investigation, and to Mr. L. E. Starr of the

Naval Ordnance Laboratory for assisting in the conduct of the test of Model DSRV-3. The industrial Department is commended for the accuracy achieved in fabricating Models DSRV-3, DSRV-3C, and DSRV-3CP. Model DSRV-3L was fabricated by the Technicon Engineering Associates of Lodi, New Jersey under the direction of Mr. Carl E. Gunther. The successful completion of this task is acknowledged.

## APPENDIX

### HYDROSTATIC TEST OF A SMALL STIFFENED ALUMINUM CYLINDER

Prior to the work summarized in this report, an exploratory test was conducted on a 1.75-in.-diameter stiffened cylinder to determine the applicability of available theories of collapse for shells with closely spaced frames and of a strain-hardening material at pressures in excess of 10,000 psi. The model, designated DSRV-P, was machined from a solid bar of 7075-T6 aluminum which had a compressive yield strength of 81,000 psi. A sketch of Model DSRV-P is shown in Figure 17, and a typical stress-strain curve for the material used is shown in Figure 18.

Model DSRV-P collapsed at a pressure of 12,400 psi. A photograph of the model after collapse is shown in Figure 19.

It can be seen from Table 3 that Formulas [92]<sup>8</sup> and [92A]<sup>8</sup> predict collapse pressures well below the observed collapse pressure. The TMB plastic-hinge theory<sup>9</sup> also gives collapse pressure below the experimental collapse pressure. Since the geometry involved is very stable and, therefore, a good deal of strain hardening occurred before collapse, theories such as these, which depend on an arbitrary yield strength as that obtained by the 0.2-percent-offset method, cannot be expected to apply. The elastic collapse pressures predicted by Kendrick<sup>10</sup> (general instability), Formula [9]<sup>11</sup> (asymmetric shell buckling), and Lunchick<sup>12</sup> (axisymmetric shell buckling) are well above the observed collapse pressure. The available theories of Reynolds<sup>13</sup> and Lunchick<sup>12</sup> for collapse

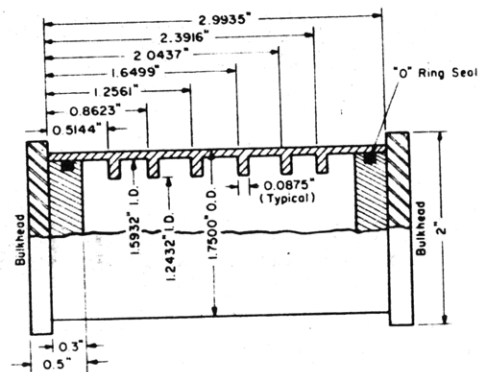


Figure 17 - Model DSRV-P

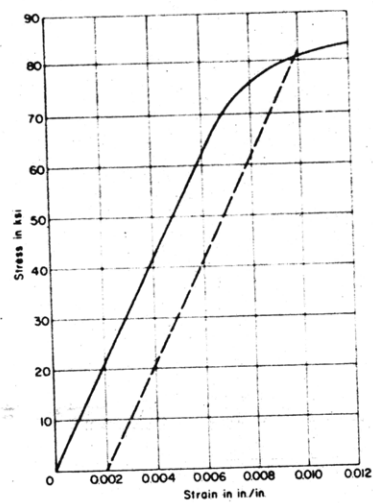
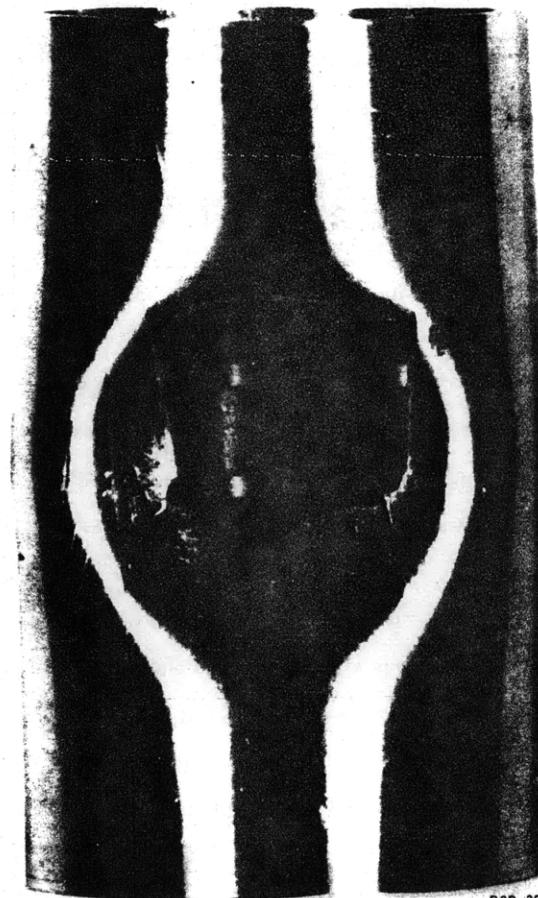


Figure 18 - Typical Stress-Strain Curve for Material Used in Model DSRV-P



PSD 301082

Figure 19 - Model DSRV-P after Collapse

TABLE 3

Ratio of Theoretical Collapse Pressure to Experimental  
Collapse Pressure for Model DSRV-P

Theory of Collapse	Theoretical Collapse Pressure Experimental Collapse Pressure
Formula [92] <sup>8</sup>	0.82
Formula [92A] <sup>8</sup>	0.80
TMB Plastic Hinge <sup>9</sup>	0.91
Kendrick Part III <sup>10</sup>	3.3
EMB Formula [9] <sup>11</sup>	7.2
Elastic Axisymmetric Shell Buckling <sup>12</sup>	8.0
Reynold's Plastic Asymmetric Shell Buckling <sup>13</sup>	> 1.1
Lunchick's Plastic Axisymmetric Shell Buckling <sup>12</sup>	> 1.1
Plastic General Instability, Formula 1	0.95
Plastic General Instability, Formula 9	0.96

by plastic asymmetric and axisymmetric shell buckling, respectively, also give pressures above the experimental collapse pressure.

The appearance of Model DSRV-P after failure (see Figure 19) suggests that it may have collapsed by plastic general instability. Unfortunately, no theory existed for this mode of collapse at the time of this test.

Therefore, the following approximations for the plastic general instability collapse strength were developed.\*

The assumption that the plastic general-instability strength of a long, stiffened cylinder is analogous to the plastic buckling strength of a column<sup>15</sup> leads to the following approximation of the plastic general-instability collapse pressure  $p_t$ :

$$p_t = \frac{E_t}{E} P_{cr} \quad [1]$$

where  $E$  is Young's modulus,

$E_t$  is the tangent modulus at the critical stress level, and

$P_{cr}$  equals the elastic general-instability pressure as predicted by Bryant<sup>16</sup> when modified to consider only the effective width of shell and the internal or external position of the stiffener.

For sufficiently close frame spacing, the average circumferential stress  $\sigma_\phi$  may be approximated by

$$\sigma_\phi = \frac{p R_o}{h + A_s/L_f} \quad [2]$$

where  $p$  is the applied pressure,

$R_o$  is the outside radius,

$h$  is the shell thickness,

$A_f$  is the cross-sectional area of the frame, and

$L_f$  is the distance between frame centers.

\* Lunchick presents a more rigorous solution to this problem in Reference 14.

The longitudinal stress  $\sigma_x$  may be approximated by

$$\sigma_x = \frac{p R_o}{2h} \quad [3]$$

and the radial stress  $\sigma_r$  by

$$\sigma_r = 0 \quad [4]$$

If the Hencky-Von Mises yield criterion<sup>2</sup> is assumed to apply in the plastic range, the stress-strain relationship between the model and a simple compression specimen may be expressed in terms of the stress intensity  $\sigma_i$  defined as

$$\sigma_i = \left[ \sigma_\phi^2 + \sigma_x^2 - \sigma_\phi \sigma_x \right]^{1/2} \quad [5]$$

The plastic general-instability collapse pressure  $p_t$  can now be estimated as follows: From a representative stress-strain curve of the material used in the cylinder,  $E_t/E$  may be defined in terms of  $\sigma_i$  and, therefore,  $p_t$  can be plotted as a function of  $\sigma_i$  by using Equation [1]. Similarly, the applied pressure  $p$  can be plotted against  $\sigma_i$  as determined by Equation [5];  $p_t$  corresponds to the intersection of the two curves.

Bryant's expression for the general-instability collapse pressure  $P_B$ <sup>16</sup> is composed of two terms:

$$P_B = P_s \left( \frac{L_b}{R}, \frac{h}{R}, n \right) + P_f \left( \frac{I}{L_f R^3}, n \right) \quad [6]$$

where  $P_s$  is associated with the strength of the unstiffened shell,  
 $P_f$  is associated with the strength of frame per unit length of shell,

$L_b$  is the bulkhead spacing,

$n$  is the number of circumferential waves,

$I$  is the moment of inertia about the centroid of a section comprising one frame plus a length of shell equal to one frame spacing, and

$R$  is the radius to the midplane surface of the shell.

Modifying the second term in Equation [6] to consider only the effective width of shell and the internal or external position of the stiffener yields the following expression for the elastic general-instability collapse pressure

$$P_{cr} = \frac{Eh}{R} \left[ \frac{\lambda^4}{(n^2 + \frac{\lambda^2}{2} - 1)(n^2 + \lambda^2)^2} \right] + \frac{EI_e (n^2 - 1)}{L_f R_o R_c^2} \quad [7]$$

where

$$\lambda = \frac{\pi R}{L_b},$$

$I_e$  is the moment of inertia about the centroid of a section comprising one frame plus an effective length of shell, and

$R_c$  is the radius to neutral axis of the frame, effective shell combination.

The effective length of shell  $L_e$  may be determined by

$$L_e = F_1 (L_f - b) + b \quad [8]$$



where  $b$  is the width of web in contact with the shell,

$$F_1^* = \frac{2}{\theta} \left[ \frac{\cosh^2 \frac{\theta}{2} - \cos^2 \frac{\theta}{2}}{\cosh \frac{\theta}{2} \sinh \frac{\theta}{2} + \cos \frac{\theta}{2} \sin \frac{\theta}{2}} \right], \text{ and}$$

$$\theta = \frac{[3(1 - \nu^2)]^{1/4} [L_f - b]}{(Rh)^{1/2}}$$

Since the plastic buckling of an unstiffened cylinder<sup>18</sup> under uniform pressure is a function of the secant modulus  $E_s$  as well as the tangent modulus,\*\* Equation [1] may yield slightly conservative pressures when applied to relatively short ring-stiffened cylinders. Therefore, the following expression can be used to predict the plastic general-instability collapse pressure  $p_{st}$  of short as well as long ring-stiffened cylinders.

$$p_{st} = \left[ E_s E_t \right]^{1/2} \frac{h}{R} \left[ \frac{\lambda^4}{(n^2 + \frac{\lambda^2}{2} - 1)(n^2 + \lambda^2)^2} \right] + \frac{E_t I_e}{L_f R_o R_c^2} (n^2 - 1) \quad [9]$$

Applying Equations [1] and [9] to Model DSRV-P gives collapse pressures  $p_t$  and  $p_{st}$  of 95 and 96 percent of the experimental collapse pressure, respectively.

\*  $F_1$  may be determined graphically from Reference 17.

\*\* For the purpose of this analysis, the plasticity reduction factor for moderate length cylinders obtained by Gerard<sup>18</sup> may be adequately approximated by  $\left[ \frac{E_s E_t}{E^2} \right]^{1/2}$ .

## REFERENCES

1. Timoshenko, S., "Strength of Materials - Part II," Second Edition, D. Van Nostrand Company, Inc., New York (1941).
2. Seely, F. and Smith, V., "Advanced Mechanics of Materials," Second Edition, John Wiley and Sons, Inc., New York (1955).
3. Short, R. D., "Membrane Design for Stiffened Cylindrical Shells Under Uniform Pressure," David Taylor Model Basin Report (in preparation).
4. Krenzke, M. A., "Hydrostatic Tests of Conical Reducers between Cylinders with and without Stiffeners at the Cone-Cylinder Juncture," David Taylor Model Basin Report 1187 (Feb 1959).
5. Bijlaard, P. P., "Theory and Tests on the Plastic Stability of Plates and Shells," Journal of the Aeronautical Sciences, Vol. 16, No. 9 (Sep 1949).
6. Krenzke, M. A., "Tests of Machined Deep Spherical Shells under External Hydrostatic Pressure," David Taylor Model Basin Report 1601 (May 1962).
7. Willner, A. R. and Sullivan, V. E., "Progress Report - Metallurgical Investigators of Titanium Alloys for Application to Deep-Diving Submarines," David Taylor Model Basin Report 1482 (Dec 1960).
8. Von Sanden, K. and Gunther, K., "The Strength of Cylindrical Shells, Stiffened by Frames and Bulkheads, under Uniform External Pressure on All Sides," David Taylor Model Basin Translation 38 (Mar 1952).

9. Lunchick, M. E., "Yield Failure of Stiffened Cylinders under Hydrostatic Pressure," David Taylor Model Basin Report 1291 (Jan 1959).
10. Kendrick, S., "The Buckling under External Pressure of Circular Cylindrical Shells with Evenly Spaced Equal Strength Circular Ring Frames - Part III," Naval Construction Research Establishment Report NCRE/R.244 (Sep 1953).
11. Windenburg, D. F. and Trilling, C., "Collapse by Instability of Thin Cylindrical Shells under External Pressure," Experimental Model Basin Report 385 (Jul 1934).
12. Lunchick, M. E., "Plastic Axisymmetric Buckling of Ring-Stiffened Cylindrical Shells Fabricated from Strain-Hardening Materials and Subjected to External Hydrostatic Pressure," David Taylor Model Basin Report 1393 (Jan 1961).
13. Keynolds, T. E., "Inelastic Lobar Buckling of Cylindrical Shells under External Hydrostatic Pressure," David Taylor Model Basin Report 1392 (Aug 1960).
14. Lunchick, M. E., "Plastic General Instability of Ring-Stiffened Cylindrical Shells," David Taylor Model Basin Report 1587 (Sep 1963).
15. Bleich, Frederick, "Buckling Strength of Metal Structures," McGraw-Hill Book Company, Inc., New York (1952).
16. Bryant, A. R., "Hydrostatic Pressure Buckling of a Ring-Stiffened Tube," Naval Construction Research Establishment Report R306 (1954).

17. Krenzke, M. A. and Short, R. D., "Graphical Method for Determining Maximum Stresses in Ring-Stiffened Cylinder under External Hydrostatic Pressure," David Taylor Model Basin Report 1348 (Oct 1959).
18. Gerard, G., "Plastic Stability Theory of Thin Shells," Journal of the Aeronautical Sciences, Vol. 24, No. 4 (Apr 1957).

MIT LIBRARIES

DUPL



3 9080 02754 4383

APR 15 1974

OCT 7 1986